# Impact of Classical and Quantum Light on Donor-Acceptor-Donor Molecules

Haraprasad Mandal,<sup>[1]†</sup> Sajal Kumar Giri,<sup>[2]†</sup> Sara Jovanovski,<sup>[1]</sup> Oleg Varnavski,<sup>[1]</sup> Malgorzata Zagorska,<sup>[3]</sup> Roman Ganczarczyk,<sup>[3]</sup> Tse-Min Chiang,<sup>[4]</sup> George C. Schatz,<sup>[3,4]</sup> Theodore Goodson,

III<sup>[1]\*</sup>

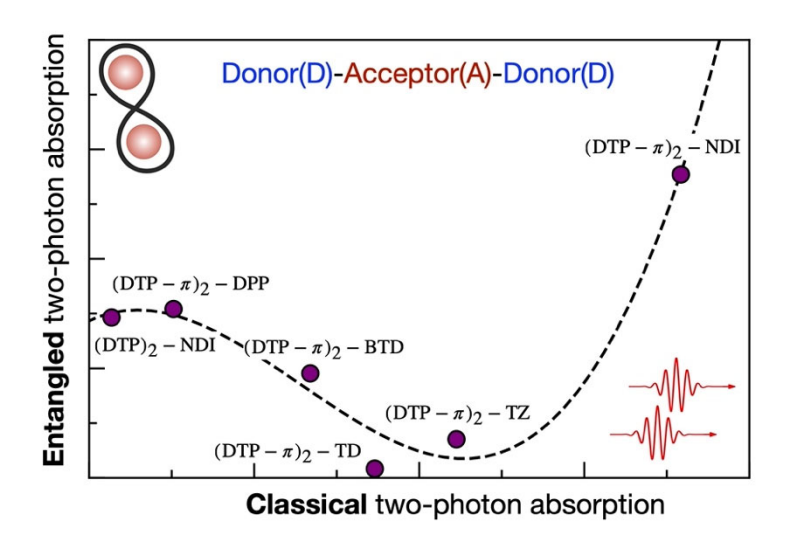
## **AUTHOR ADDRESS**

- [1] Department of Chemistry, University of Michigan, Ann Arbor, Michigan 48109, United States
- [2] Department of Chemistry, Northwestern University, Evanston, Illinois 60208, United States
- [3] Faculty of Chemistry, Warsaw University of Technology, Noakowskiego 3, 00-664 Warsaw, Poland
- [4] Applied Physics Program, Northwestern University, Evanston, Illinois 60208, United States
- † Equal contributions

# Abstract

Investigations of entangled and classical two-photon absorption have been carried out for six donor (D)-acceptor(A)-donor(D) compounds containing the dithieno pyrrole (DTP) unit as donor and acceptors with systematically varied electronic properties. Comparing ETPA (quantum) and TPA (classical) results reveals that the ETPA cross section decreases with increasing TPA cross section for molecules with highly off-resonant excited states for single photon excitation. Theory (TDDFT) results are in semiquantitative agreement with this anticorrelated behavior, due to the dependence of the ETPA cross section but not TPA on the two-photon excited state lifetime. The largest cross section is found for a DTP derivative that has a single photon excitation energy closest to resonance with half the two-photon excitation energy. These results are important to the possible use of quantum light for low intensity energy conversion applications.

# **Table of Content (TOC)**



A quest for cost-effective materials within the realm of optoelectronics, electrochromic and solar devices has captivated the interest of researchers and innovators alike. Organic materials show promising qualities that the scientific community may consider as potential replacements for organometallic phosphor counterparts for energy conversion and there is also interest in their two-photon absorption (TPA) properties. Different aspects of the photophysics of organic materials important for photovoltaic applications (such as TPA upconversion) have been explored but their interaction with non-classical states of light have received little attention. Non-classical light spectroscopy, such as entangled two-photon absorption (ETPA), can uncover new details in the photophysics due to the unique capabilities of entangled light.

ETPA, discovered theoretically <sup>5-8</sup> and later experimentally <sup>9-16</sup> proven efficient for two-photon excitation of organic chromophores, has become a novel technique for studying nonlinear properties of organic molecules using quantum light. The generation of entangled photons can be done using spontaneous parametric down-conversion (SPDC) (see the SI for more details).<sup>17,18</sup> Early theory work predicted that there would be a linear incident light intensity dependence of the absorption rate on the entangled photon pair flux,<sup>6</sup> and this was confirmed experimentally later with atomic<sup>19</sup> and molecular<sup>9</sup> targets. This linear photon intensity dependence of ETPA (compared to the quadratic dependence of TPA) enables the required intensity for measurements to be orders of magnitude lower compared to TPA.<sup>20-22</sup> Therefore, TPA is restricted by necessity to high power sources<sup>23</sup> while ETPA can be used for sensitive samples potentially prone to photodamage such as living cells.<sup>22</sup> Moreover, ETPA shows promise as a novel tool for spectroscopic and imaging applications, in general.<sup>24-29</sup> However, various details of the ETPA absorption mechanism are still under debate.<sup>8,15,19,30-34</sup> The values of the ETPA cross-sections for organic molecules reported in the literature lie in a broad range 10<sup>-18</sup> - 10<sup>-25</sup> cm<sup>2 33,35</sup> down to those below the detection limit of the

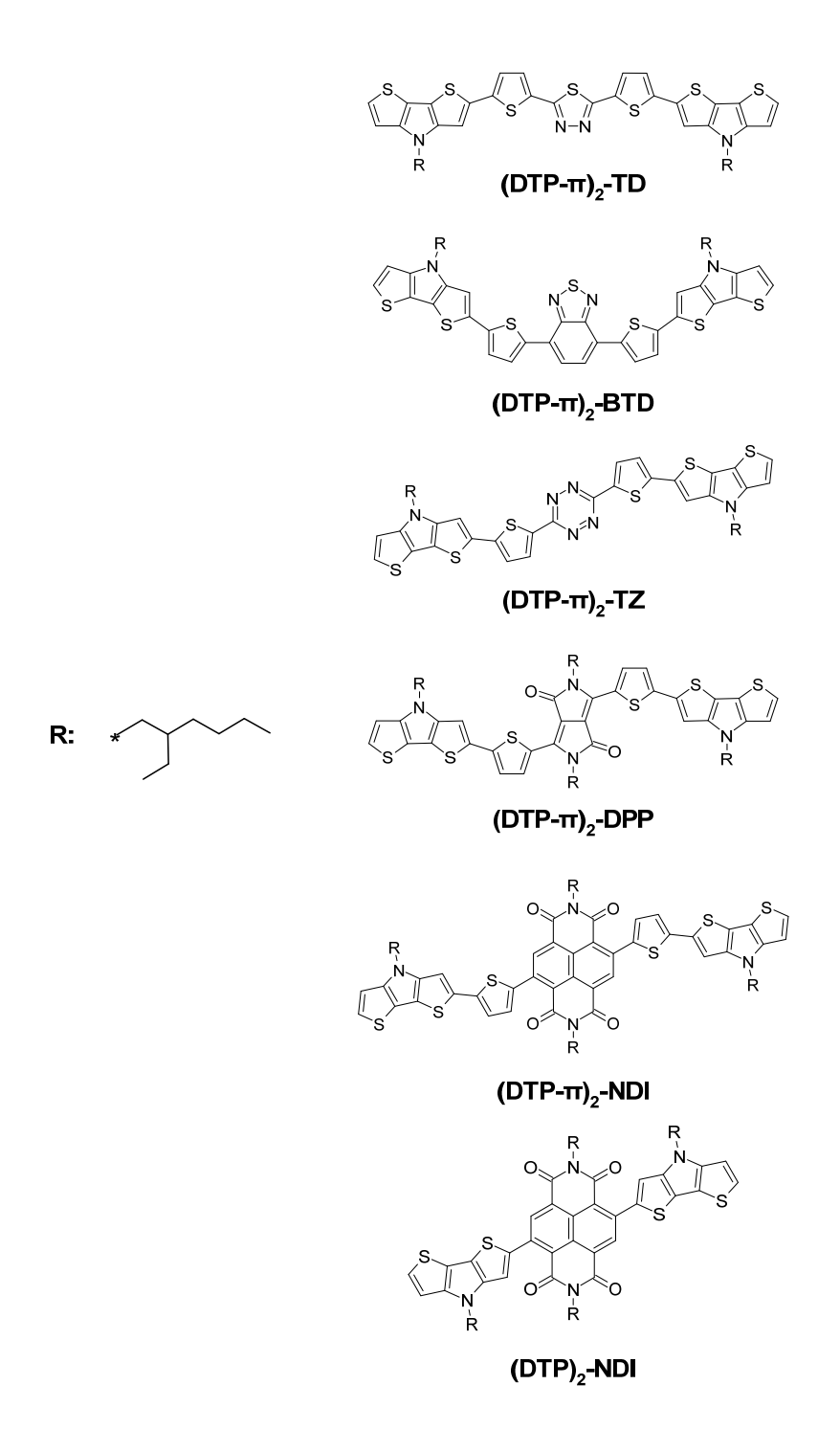
setup. <sup>33, 34, 36</sup> Experimentally, it is challenging to clearly distinguish one–photon processes (such as scattering, <sup>32,33, 37</sup> and hot band absorption <sup>38</sup>) from the linear dependent and relatively weak true ETPA in direct transmission and fluorescence measurements. <sup>31-34,37</sup> Various approaches directed at the detection of the specific features of ETPA not inherent in one photon processes, have also been used to better characterize the ETPA. Among them are investigations of spatial ETPA properties, <sup>11,15,26</sup> methods exploring the spectral width of the ETPA signal, <sup>26</sup> using different attenuation schemes affecting photon statistics (pump attenuation vs entangled beam attenuation), <sup>15</sup> exploring specific time dependence of ETPA excited fluorescence, <sup>12,14,16, 21</sup> as well as measuring the ETPA spectrum and the absence of the absorption signal after spectral selection of a single photon from the pair. <sup>39</sup> These observations taken together are not compatible with single photon absorption or scattering processes. Instead they have demonstrated the presence of specific ETPA features in experiments.

Among organic molecules, donor-acceptor-donor (D-A-D) compounds have attracted noticeable attention, with highly tunable electronic properties that can readily be determined by organic synthesis. As examples of this, we consider five D- $\pi$ -A- $\pi$ -D compounds and one D-A-D compound based on the DTP (dithieno [3,2-b:2',3'-d] pyrrole) donor pictured in Figure 1 (see Fig. S1 and Table S3 for optimized geometries). Here the five D- $\pi$ -A- $\pi$ -D compounds have DTP attached to an acceptor central unit of varying electron withdrawing properties through a  $\pi$ -linker (2,5-thienylene). In a sixth compound, (DTP)<sub>2</sub>-NDI, the donor units are directly linked to the central acceptor core.

Given that the DTP derivatives provide molecules with systematically tunable electronic properties, it is of interest to study structure-function relationships when these molecules interact with light, and especially with quantum light leading to ETPA. Although there have been many ETPA studies in the past decade, none of these have so-far revealed systematic variation of ETPA cross

sections with molecular electronic properties, which means that property optimization of ETPA is not understood. Since TPA and ETPA can be characterized by numerical cross section values which are crucial for observations it is imperative to understand and optimize trends in these cross sections as molecular properties are systematically varied. Here we study possible trends for all the abovementioned DTP compounds, using experiments and electronic structure theory for both TPA and ETPA.

Here, we have investigated the TPA and ETPA optical properties (SI Section S1 for experimental details) of the six DTP compounds including a determination of the classical and entangled two-photon absorption cross sections. One-photon absorption (OPA) results are also compared, and for all measurements we present results from TDDFT calculations (SI Section S2 for theoretical and computational details) based on a recently developed theory<sup>30,39</sup> to interpret the trends that are presented by the six molecules. Indeed, the comparisons of theory and experiment provide important tests of the theory for a series of molecules where TPA and ETPA cross sections do not scale in the same way as the electronic properties are systematically varied.



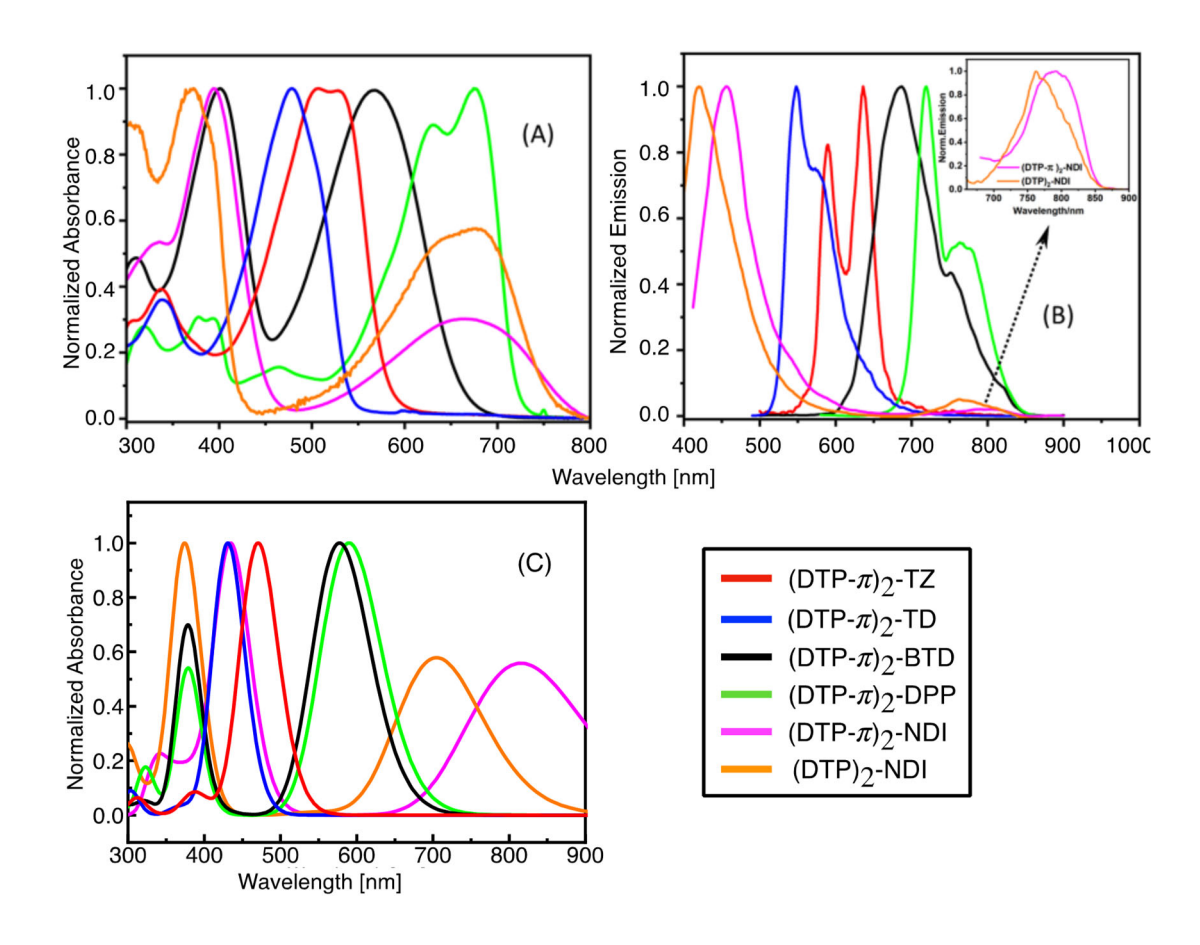
**Figure 1.** Molecular structure of studied D-A-D compounds. Throughout we group  $(DTP-\pi)_2$ -NDI and  $(DTP)_2$ -NDI as pair A,  $(DTP-\pi)_2$ -BTD and  $(DTP-\pi)_2$ -DPP as pair B, and  $(DTP-\pi)_2$ -TD and  $(DTP-\pi)_2$ -TZ as pair C. A detailed explanation is given in the main text for such pairing.

Figure 2A shows one-photon absorption (OPA) spectra of all DTP compounds in toluene at room temperature and the absorption maxima are recorded in Table 1. All the spectra seen here cannot be explained by a simple superposition of the spectrum of dithienopyrrole (DTP) with alkyl Nsubstituent and the corresponding spectra of compounds that replicate the  $\pi$ -A- $\pi$  unit of the studied molecules, such as thiadiazole (TD), benzothiadiazole (BTD), diketopyrrolopyrrole (DPP), tetrazine (TZ), and naphthalene diimide (NDI) disubstituted with thienyl groups. N-alkylated DTP produces a strong vibronic band character with a clear maximum at 300 nm corresponding to the dominant 0-1 transition. 40 This vibronic band is either non-existent or significantly altered in the investigated compounds. In addition, in the spectra of the investigated derivatives, the absorption bands with the lowest energy predominate and are strongly red-shifted relative to analogous bands in the spectra of compounds similar to the  $\pi$ -A- $\pi$  segments of the investigated molecules. For example, (DTP- $\pi$ )<sub>2</sub>-NDI has the most red-shifted absorption band (the smallest band-gap) in comparison with the other DTP compounds. Furthermore, (DTP)<sub>2</sub>-NDI, an analogue of (DTP- $\pi$ )<sub>2</sub>-NDI without the  $\pi$ linker, exhibits a similar red-shifted absorption band. Naphthalene diimides core-functionalized with donors of different strengths exhibit very characteristic UV-vis spectra. In this case, the band with the lowest energy is a CT band, while the most intense band is situated at shorter wavelengths. 41,42 In the spectra of  $(DTP-\pi)_2$ -NDI and  $(DTP)_2$ -NDI both the CT and intense bands are strongly red shifted with respect to the corresponding bands in N,N'-bis(2-ethylhexyl)-2,6-dithiophene-1,4,5,8naphthalene diimide, 43 i.e., a molecule similar to the D-A-D segment of  $(DTP-\pi)_2$ -NDI and (DTP)<sub>2</sub>-NDI. Thus, by comparing the UV-vis spectra of the D-A-D compounds studied in this research with the corresponding spectra of the compounds that are similar to their central  $\pi$ -A- $\pi$  or A segment, it can be concluded that the observed red shift of the lowest energy band is due to two

factors: extension of the  $\pi$ -system and donor-acceptor interactions. A stronger D-A interaction is responsible for a more pronounced red shift which increases with increasing acceptor strength.

The computational results (details in SI Section S2) in Figure 2C show absorption spectra that are generally in good agreement with the experimental results, but subject to the usual errors in TDDFT energies that can be on the order of 0.1-0.2 eV. Solvation effects can also contribute. What we see is that the lowest energy excitations occur close to 700-800 nm for (DTP- $\pi$ )<sub>2</sub>-NDI and (DTP)<sub>2</sub>-NDI, then 600-700 nm for (DTP- $\pi$ )<sub>2</sub>-DPP and (DTP- $\pi$ )<sub>2</sub>-BTD, then 400-500 nm for (DTP- $\pi$ )<sub>2</sub>-TZ and (DTP- $\pi$ )<sub>2</sub>-TD. Based on these trends and later results for TPA and ETPA, we have grouped the molecules into three pairs, which we label as pair A ((DTP- $\pi$ )<sub>2</sub>-NDI and (DTP)<sub>2</sub>-NDI), B (DPP and BTD) and C (TZ and TD). These pairings will provide a useful way to discuss the two-photon results below.

To provide further insights, we performed fluorescence emission experiments by exciting  $(DTP-\pi)_2$ –TD at 477 nm,  $(DTP-\pi)_2$ –BTD at 407 nm,  $(DTP-\pi)_2$ –DPP at 630 nm,  $(DTP-\pi)_2$ –TZ at 520 nm,  $(DTP-\pi)_2$ –NDI at 400 nm and  $(DTP)_2$ –NDI at 370 nm respectively. As shown in Figure 2B, the emission spectra for all the studied molecules range from 500 nm to 900 nm. Like absorption spectra, the emission bands are also progressively redshifted with increasing acceptor strength from  $(DTP-\pi)_2$ –TD to  $(DTP-\pi)_2$ –NDI. All steady state results (emission peaks and fluorescence quantum yields) are listed in Table 1. As one can see in Table 1, with increasing the acceptor strength, the Stokes shift also increases, while the photoluminescence quantum yield strongly decreases. However, for  $(DTP-\pi)_2$ –NDI, and  $(DTP-\pi)_2$ –TZ, quantum yields smaller than 1% were obtained. The large Stokes shifts for these molecules indicate that the geometries of the molecules in their excited state significantly differ from those of the ground state giving rise to strong dipole moment differences for these molecules.



**Figure 2**. Steady-state (A) absorption and (B) emission spectra of  $(DTP-\pi)_2-TD$ ,  $(DTP-\pi)_2-BTD$ ,  $(DTP)_2-NDI$ ,  $(DTP-\pi)_2-DPP$ ,  $(DTP-\pi)_2-TZ$  and  $(DTP-\pi)_2-NDI$  in toluene at room temperature. (C) Absorption spectra using TDDFT calculations.

**Table 1**. Steady-state results for one-photon absorption and emission for all D-A-D compounds in toluene.

Compounds	$\lambda_{abs}^{max}$ (nm)		$\lambda_{emi}^{max}$ (nm)	Fluorescence Quantum	
	Expt.	Theory		Yield (%)	
$(DTP-\pi)_2$ -TD	<u>477</u>	431	<u>543</u> , 578	64	
(DTP-π) <sub>2</sub> -BTD	<u>407</u> , 565	378, 577	<u>687</u>	49.4	
(DTP-π) <sub>2</sub> -DPP	<u>630</u> , 674	590	<u>718</u> , 767	15	
(DTP) <sub>2</sub> -NDI	<u>370</u> , 650	387, 705	<u>418</u> , 763	1.65	
$(DTP-\pi)_2$ -TZ	<u>520</u>	470	<u>590</u> , 637	0.0134	
(DTP-π) <sub>2</sub> -NDI	<u>405</u> , 687	432, 815	<u>477</u> , 790	0.095	

The underlined wavelengths indicate the excitation and detection wavelengths for fluorescence quantum yield measurement.

We have investigated the non-linear absorption of DTP derivatives by using the two-photon excited fluorescence (TPEF) method. An excitation wavelength of 800 nm (for (DTP-π)<sub>2</sub>-NDI, (DTP- $\pi$ )<sub>2</sub>-TD, (DTP- $\pi$ )<sub>2</sub>-TZ and (DTP)<sub>2</sub>-NDI) and 820 nm (for (DTP- $\pi$ )<sub>2</sub>-DPP and (DTP- $\pi$ )<sub>2</sub>-BTD) were used to perform the experiment (details are given in the SI Section S1). Firstly, the emission intensity with respect to the excitation power was collected to confirm the quadratic dependence with respect to the excitation power. In this non-linear optical experiment, the quadratic dependence signal is an important parameter to verify in order to avoid an over-estimation of the TPA cross section due to OPA. The logarithmic plot of the intensity (counts per second) versus the laser power (mW) shows a linear fit with a slope of 1.8 to 2.0 for all studied samples (Figure S2A for linear fit and Table 2 for cross section) indicating quadratic dependence for all the studied samples. The standard deviation for these slopes was found to be in the range between  $\pm 0.07$  to  $\pm 0.02$ . These standard deviations are attributed to the instrument's response function or to certain corrective variables. The two-photon power-dependence was used to calculate the two-photon absorption cross section. Coumarin 307 (for (DTP- $\pi$ )<sub>2</sub>-NDI, (DTP- $\pi$ )<sub>2</sub>-TD, (DTP- $\pi$ )<sub>2</sub>-DPP and (DTP- $\pi$ )<sub>2</sub>-BTD), 9chloroanthracene (for DTP)<sub>2</sub>-NDI) and rhodamine 6G (for (DTP-π)<sub>2</sub>-TZ) were used as the TPA standard (std) to compute the TPA cross sections. The TPA cross sections were calculated using the following equation:

$$\sigma_{sample} = \frac{{{10}^{b}}sample^{-b}std}{\phi_{std}\sigma_{std}[c]_{std}n_{std}}}{\phi_{sample}[c]_{sample}n_{sample}}$$

where  $\phi$  is the emission quantum yield, n is the solvent refractive index, b is the intercept in the linear fit of the quadratic power dependence, and [c] is the concentration. The two-photon

photoluminescence spectra for all DTP derivatives were collected at their emission maxima. The two-photon excited fluorescence spectra of (DTP- $\pi$ )<sub>2</sub>–TD, (DTP- $\pi$ )<sub>2</sub>–NDI, (DTP)<sub>2</sub>–NDI and (DTP- $\pi$ )<sub>2</sub>–TZ reveals an emission maximum at 540 nm, 462 nm, 448 and 570 nm, respectively (Figure S2B). However, for (DTP- $\pi$ )<sub>2</sub>–DPP and (DTP- $\pi$ )<sub>2</sub>–BTD, the detection wavelength was 500 nm and 450 nm, respectively (inset of Figure S2B). The obtained two-photon excitation emission spectra are very similar to the one-photon steady-state emission spectra. The emission peaks closely match those of the steady state spectra (one-photon), but the two-photon emission spectra are slightly blue-shifted relative to the corresponding steady state spectra. The blue shift may be surprising because there are other symmetry-allowed two-photon transitions at a lower energy.<sup>44</sup> It is well known that the difference in the one- and two-photon absorption spectra arise from the different selection rules that these transitions have to obey. In the dipole approximation, only transitions between two states characterized by no more than one unit change in angular momentum are allowed via one-photon absorption (1PA), while different selection rules apply for 2PA, which leads to different absorption peaks in the spectra, <sup>45</sup> including symmetry-allowed two-photon transitions at lower energy.

The TPA cross sections for all DTP derivatives are listed in Table 2. (DTP- $\pi$ )<sub>2</sub>–DPP has the lowest TPA cross section value of 87.2 GM (measured), whereas the TPA cross section value for (DTP- $\pi$ )<sub>2</sub>–BTD is slightly increased to 108 GM. The (DTP- $\pi$ )<sub>2</sub>–TZ and (DTP- $\pi$ )<sub>2</sub>–TD (pair C) exhibit TPA cross-sections of 318 GM and 389 GM respectively, significantly higher than those determined for (DTP- $\pi$ )<sub>2</sub>–DPP and (DTP- $\pi$ )<sub>2</sub>–BTD (pair B). The TPA cross section determined for DTP- $\pi$ )<sub>2</sub> –NDI with the  $\pi$ -linker is 974 GM, indicating its highly pronounced intramolecular charge transfer (ICT) character and close to resonance excitation wavelength. This reflects the small bandgap for this molecule, and we will see other manifestations in the computational analysis given later when we discuss ETPA. For (DTP)<sub>2</sub>-NDI *i.e.*, the only compound without the  $\pi$ -linker, a cross

section of 115 GM was obtained. This result may seem somewhat anomalous as we might have expected a larger cross section due to similarity of the lowest excitation energy for this molecule with that for  $(DTP-\pi)_2$ –NDI (hence the pair A designation), but the TPA value for  $(DTP)_2$ -NDI is within the uncertainties of our TDDFT calculations, so the smaller value can be correlated with the lack of a  $\pi$ -linker. However at least for  $(DTP-\pi)_2$ –NDI, the NDI group provides greater acceptor contributions than the DPP and BTD units, which is in agreement with previous studies that relate donor – acceptor strength to CT character. Also, TZ and TD provide greater acceptor contribution than the NDI unit without the  $\pi$ -linker, which is in agreement with previous studies that relate donor – acceptor strength to CT character.

The TPA cross sections from TDDFT calculations are also given in Table 2. Details of the theory are given in the SI Section S2, and we note that this theory is based on the Fermi's Golden Rule. It assumes that the density of final states for ETPA is determined by the radiative lifetime of the two-photon excited states, rather than the much shorter dephasing time that is typically used for TPA. Here we provide cross sections for several possible two-photon excited states, with the results in bold indicating the result that most likely represents the experiment based on how close the two-photon energy is to the experimental energy (400 nm or 3.1 eV) as well as the largest cross section we calculated. The only ambiguous assignments arise for the TZ and TD molecules, where the states closest to 400 nm have cross sections that are much smaller than experiment. Thus, we have used states near 300 nm that have cross sections that compare more reasonably with the experimental values (with energies that are still within the accuracy expected for TDDFT calculations). The same states are also used for the calculated ETPA cross sections describe below. Table 2 shows that the measured and calculated cross sections are in good agreement (within a factor of 3), certainly at the level of quality that can be expected from TDDFT based on past works.<sup>30,39</sup> These results indicate

that the  $(DTP-\pi)_2$ -NDI member of pair A has the largest cross section, while pair C is the next largest and pair B the smallest.  $(DTP)_2$ -NDI from pair A is again anomalous, with a lower cross section than pairs B and C as noted in the paragraph above.

**Table 2**. Classical and entangled two-photon absorption results for all D-A-D compounds in toluene. In addition to the experimental results, the results of theory are also given for several choices of the two-photon excited state (details given in SI, Section S3), with the result in bold being the most likely choice.

Compounds	Experiment		Theory			
	$\delta_r$	$\sigma_e$	States	Wavelength	$\delta_r$	$\sigma_e$
	[GM]	$[10^{-19}  \text{cm}^2]$		[nm]	[GM]	$[10^{-19}  \text{cm}^2]$
(DTP-π) <sub>2</sub> –NDI	974	29.2	2>	711	100	45.4
			7>	428	112	12.8
			8>	410	1962	24.3
			10>	397	104	7.5
(DTP) <sub>2</sub> -NDI	115	10.8	2>	598	27	13.8
			4>	547	2	3.2
			7⟩	372	37	5.4
			10>	345	68	4.3
			18>	325	214	3.2
(DTP-π) <sub>2</sub> -BTD	108	3.08	2⟩	421	148	3
(DTP-π) <sub>2</sub> -DPP	87.2	3.45	2⟩	414	57	5.9
(DTP-π) <sub>2</sub> -TD	389	2.48	2>	369	16	0.2
			6⟩	300	232	1.1

$(DTP-\pi)_2-TZ$	318	2.52	3>	411	0.4	1.7
			4>	388	41	0.3
			9⟩	313	410	1.5

Entangled photon pairs at 810 nm generated by type-I SPDC were employed in these ETPA experiments. Full details of our experimental setup have been reported previously<sup>26,47</sup> and can be found in the Supporting Information. In short, a BBO crystal cut for Type I phase matching condition was pumped using 405 nm focused light from a CW diode laser. After spectral filtering the entangled photon light centered at wavelength 810nm was focused into the sample and collimated after the sample. A combination of a dichroic mirror, bandpass filter ( $\lambda_c$ =810nm  $\delta\lambda$ = 30nm), and long pass filter with the total attenuation  $10^{13.5}$  at 405nm was used to separate the entangled light from the pump beam and other spurious light (see more details in SI). The Joint Frequency Spectrum (JFS) of signal and idler beams from our SPDC and related information about degree of entanglement is provided in our previous publication.<sup>47</sup> After collimation transmitted entangle photon beam was focused on avalanche photodiode.<sup>47</sup> To obtain the ETPA rate the entangled photon transmission though the cuvette with pure solvent was compared with that from the substance solution (see SI).

The experimental setup for ETPA measurements has been characterized in detail in previous publications<sup>26, 47</sup> Among other aspects, the possible contribution of scattering processes to the detected signal was estimated<sup>47</sup> and a specific dependence of the ETPA absorption signal on the spectral width of entangled photon pair  $\sigma_I$  was measured.<sup>26</sup> Potential contribution from different types of scattering processes to the absorption signal was found to be negligible under our experimental conditions.<sup>47</sup> At the same time, the absorption of the SPDC light showed non-trivial,

non-monotonic dependence on  $\sigma_f$ .<sup>26</sup> We found that the entangled photon pair absorption initially decreases with increase in  $\sigma_f$ , then shows a peak with further increase in  $\sigma_f$ .<sup>26</sup> Moreover the spectral width dependence appeared to be very different for Type I and Type II BBO crystals used in the SPDC.<sup>26</sup> This specific entangled photon absorption behavior cannot be explained by scattering or hot band absorption contributions. On the other hand, the specific absorption behavior as a function of  $\sigma_f$  can be unambiguously rationalized by the particular dependence of the ETPA signal on entanglement time  $T_e$  ( $T_e \cong 1/\sigma_f$ ).<sup>26</sup> These results clearly demonstrate that our transmission setup measures the ETPA signal rather than losses from other linear processes. We have also estimated the potential contribution of single photon loss due to Rayleigh scattering and hot band absorption for substances used in the current paper. These contributions were found to be much smaller than the detected ETPA signal (see details below).

ETPA was detected for all compounds studied in this work (details are in the SI). There were, however, variations in how much entangled light each compound absorbs, and this can be viewed clearly in the graph of ETPA rate (Figure S3). The extent of ETPA for each molecule changes substantially with each substituent. This implies that entangled photons are responsive to the nonlinear optical changes caused by adjustments in molecular structure. ETPA and the subsequent linear ETPA character were measured with an entangled photon flux of 10<sup>7</sup> photons/s. Only the linear dependence of ETPA was observed as the excitation intensity was not high enough for the quadratic nonlinear dependence of classical TPA to be observed. Hot-band absorption (HBA) can also contribute to SPDC signals and follows certain ETPA features,<sup>38</sup> especially if the excitation source has a broad spectrum or is shifted far away from the peak of the "0–0" transition. This is a classical OPA process from the thermally populated vibrational levels of the ground electronic state. Estimates

of the HBA contribution to the results using the procedure provided in ref. 39 showed the HBA effective cross section smaller than 10<sup>-24</sup> cm<sup>2</sup> for the DTP compounds used in this work which is orders of magnitude smaller than the measured ETPA cross section.

Measured ETPA cross sections were determined from the linear ETPA rates (Figure S3), and the results are presented in Table 2, along with results from electronic structure calculations (see SI for the details of the calculations). Also, Figure 3 summarizes the ETPA versus TPA comparison by plotting ETPA versus TPA cross sections on a log scale. This shows a "check-mark" shape for both measured and calculated results in which the ETPA cross section decreases with increasing TPA in going from pair B to pair C, and then increases in going from pair C to pair A. While experiment and theory are not in precise agreement, the semi quantitative correlations are clearly the same, which provides an important test of the theory as developed by Kang et al.<sup>30</sup> and Varnavski et al.<sup>39</sup>

To understand these results, we first note that  $(DTP-\pi)_2$ -NDI has the highest ETPA cross section (measured at  $2.8\times10^{-18}$  cm<sup>2</sup>/molecule) compared to other DTP derivatives with analogous structures with a relatively smaller acceptor group linked to the DTP unit. The contribution of the HBA cross section is found to be very small ( $\sigma_{HBA} = 9.0\times10^{-25}$  cm<sup>2</sup>) than the above measured ETPA cross-section by a factor  $3.1\times10^6$  resulting in an insignificant contribution to the ETPA. The next largest ETPA cross section is associated with  $(DTP)_2$ -NDI ( $1\times10^{-18}$  cm<sup>2</sup>/molecule). Overall, the ordering of the cross sections for the three pairs is A>B>C, which is different from what we found with the TPA results which show (except for the anomalous (DTP)<sub>2</sub>-NDI result) A>C>B. The fact that NDI with the  $\pi$ -linker has the largest ETPA cross section, and NDI without the  $\pi$ -linker has the second largest, is understandable given that these molecules have OPA states that are closest to resonance, however here we see that the anomalous (DTP)<sub>2</sub>-NDI cross section for TPA does not extend to ETPA.

In SI Section S3, we present an analysis of the transitions in the six molecules that contribute to ETPA, and we find that an important issue which distinguishes ETPA cross sections from TPA cross sections is the two-photon excited state radiative lifetime  $\tau_f$  given in Eq. S7 in terms of transition moments and energy differences, and which appears in the cross section expression Eq. S6 in terms of the lineshape function. This analysis shows that the lifetimes are usually dominated by one transition, and this is usually associated with transition from the two-photon excited state to the lowest excited state. In addition, the longest lifetime is associated with the smallest value of the energy difference for the dominant transition. For the six molecules being studied, the shortest lifetimes (and smallest ETPA cross sections) are associated with the group C molecules, then group A (except for (DTP)<sub>2</sub>–NDI) then B. This leads to a reversal in the ordering of B and C in the TPA results, leading to the observed A>B>C in the ETPA cross sections.

It has been noted that single photon loss due to Rayleigh scattering (RS) can also be important in what is measured in the ETPA experiments.<sup>37</sup> To study this possibility, we have calculated the Rayleigh scattering cross section for the six molecules we consider. The results (Fig. S7) show that Rayleigh contributions are systematically smaller than the measured results. The RS results are not completely negligible, for example the ratio of cross sections is ETPA/RS = 389 (for the experimental ETPA cross section) for the (DTP- $\pi$ )<sub>2</sub>-NDI molecule.

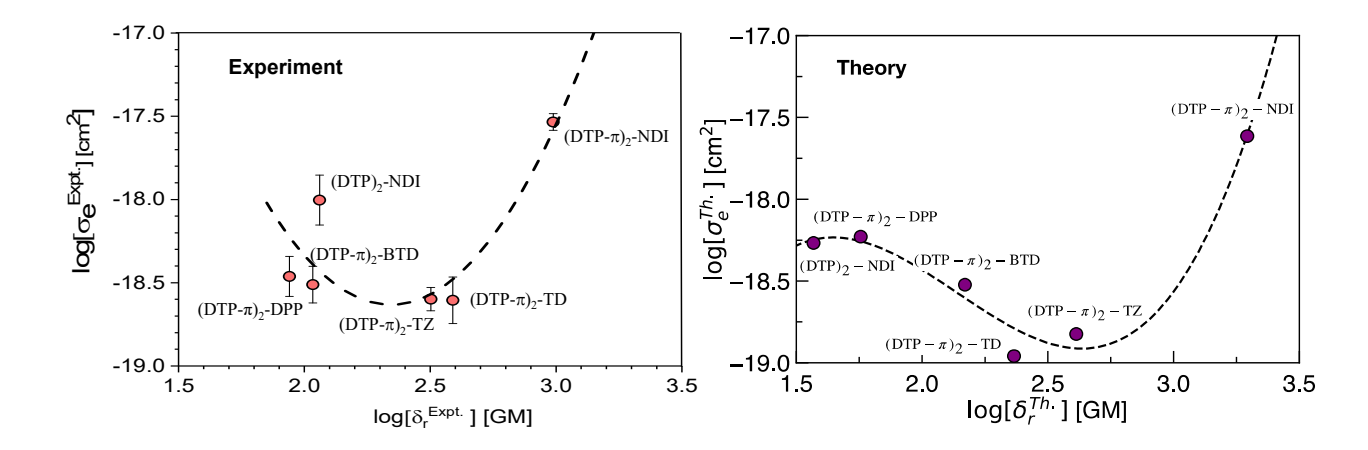


Figure 3. Log of ETPA cross section  $(\sigma_e)$  versus log of TPA cross section  $(\delta_r)$  for the DTP molecules, with the experimental results on the left and the computational results on the right. The dashed lines are polynomial fits.

In conclusion, the present comprehensive experimental and theoretical studies of the DTP derivatives show that the molecules have two-photon absorption properties that vary systematically with their electronic structure. (DTP-π)<sub>2</sub>-NDI has larger TPA and ETPA cross sections than all other DTP derivatives, due to efficient intramolecular charge transfer excitation to a low-lying state. Particularly for ETPA, this molecule can be considered as a promising candidate for two-photon energy conversion with entangled photons. More generally we find that the DTP ETPA cross sections do not follow the same trends as in classical TPA as is clearly revealed in Figure 3, implying that these molecules have different entangled light absorption trends than with classical light. We were able to explain the trends based on our recently developed ETPA theory in combination with electronic structure calculations, where excited state radiative lifetimes are found to be important in differentiating ETPA from TPA. Further we have correlated the lifetime differences to the excited state energy differences and transition dipole properties of the molecules. Together, these criteria

should enable predicting additional molecules with large ETPA cross sections for applications in

many fields.

ASSOCIATED CONTENTS

**Supporting Information** 

The supporting information is available free of charge at:

Experimental Section (sample preparation, steady-state one-photon measurements, classical two-

photon absorption, entangled two-photon absorption)

Theoretical and Computational Section (classical two-photon absorption, entangled two-photon

absorption, and Rayleigh scattering)

Analysis of ETPA Lifetimes

Supplementary Figures and Tables (optimized molecular geometries, two-photon power dependence

and fluorescence, ETPA absorption rate, transition dipole matrices, selected molecular orbitals,

energy levels and transition dipoles for emission, radiative lifetimes, spontaneous emission rates,

cartesian coordinates of optimized structures)

**AUTHOR INFORMATION** 

**Corresponding Author** 

\*Theodore Goodson, III. Email: tgoodson@umich.edu

**ORCID** 

Haraprasad Mandal: 0000-0002-5745-1844

19

Sajal Kumar Giri: 0000-0001-9145-6801

Sara Jovanovski : 0000-0003-4355-7151

Oleg Varnavski: 0009-0003-2383-9060

Tse-Min Chiang: 0009-0009-2983-0001

George C. Schatz: 0000-0001-5837-4740

Theodore Goodson, III: 0000-0003-2453-2290

## **Author Contributions**

† H. M. and S. K. G contributed equally. This manuscript was written through contributions of all

authors. All authors have given approval to the final version of the manuscript.

#### **Notes**

The authors declare no competing financial support.

ACKNOWLEDGMENTS

T.G. III acknowledges support from the US Air Force Office of Scientific Research in the Biophysics

Program via grant FA9550-20-1-0380, and from the NSF through Grant 2004076. TGIII, SKG and

GCS acknowledge the Department of Energy, Biological and Environmental Research, under grant

DE-SC0022118 for computational applications. TMC and GCS acknowledge NSF Grant CHE-

2055565 for theory development. RG and MZ acknowledge financial support from the National

Science Centre of Poland, NCN, Grant No. 2019/33/B/ST5/00582. We also thank Professor Adam

Pron for helpful discussion and critical review of the manuscript.

20

#### References

- Rybakiewicz-Sekita, R.; Toman, P.; Ganczarczyk, R.; Drapala, J.; Ledwon, P.; Banasiewicz, M.; Skorka, L.; Matyjasiak, A.; Zagorska, M.; Pron, A. D-A-D compounds combining dithienopyrrole donors and acceptors of increasing electron-withdrawing capability: Synthesis, spectroscopy, electropolymerization, and electrochromism. *J. Phys. Chem. B* 2022, 126, 4089–4105.
- 2. Vazquez, R. J.; Yun, J. H.; Muthike, A. K.; Howell, M.; Kim, H.; Madu, I. K.; Kim, T.; Zimmerman, P.; Lee, J. Y.; Goodson, T., III. New direct approach for determining the reverse intersystem crossing rate in organic thermally activated delayed fluorescent (TADF) emitters. *J. Am. Chem. Soc.* **2020**, *142*, 8074–8079.
- 3. Ye, C.; Zhou, L.; Wang, X.; Liang, Z. Photon upconversion: from two-photon absorption (TPA) to triplet–triplet annihilation (TTA). *Phys. Chem. Chem. Phys.* **2016**, *18*, 10818-10835.
- 4. Dorfman K. E.; Schlawin, F.; Mukamel, S. Nonlinear Optical Signals and Spectroscopy with Quantum Light. *Rev. Mod. Phys.* **2016**, *88*, 045008.
- 5. F. Schlawin, K.E. Dorfman, B.P. Fingerhut, S. Mukamel, Suppression of population transport and control of exciton distributions by entangled photons, *Nat. Commun.*, **2013**, *4*, 1782.
- 6. Gea-Banacloche, J., Two-photon absorption of nonclassical light. *Phys. Rev. Lett.* **1989**, *62*, 1603.
- 7. Javanainen, J.; Gould, P. L. Linear intensity dependence of a two-photon transition rate. *Phys. Rev. A* **1990**, *41*, 5088.
- 8. Fei, H.-B.; Jost, B. M.; Popescu, S.; Saleh, B. E. A.; Teich, M. C. Entanglement-induced two-photon transparency. *Phys. Rev. Lett.* **1997**, *78*, 1679.
- 9. Lee, D.-I.; Goodson, T., III. Entangled photon absorption in an organic porphyrin dendrimer. *J. Phys. Chem. B* **2006**, *110*, 25582.
- 10. Harpham, M. R.; Süzer, O.; Ma, C.-Q.; Bäuerle, P.; Goodson, T. Thiophene dendrimers as entangled photon sensor materials. *J. Am. Chem. Soc.* **2009**, *131*, 973.
- 11. Guzman, A. R.; Harpham, M. R.; Süzer, O.; Haley, M. M.; Goodson, T., III. Spatial control of entangled two-photon absorption with organic chromophores. *J. Am. Chem.*

- Soc. **2010**, 132, 7840.
- 12. Varnavski, O.; Pinsky, B.; Goodson, T., III. Entangled photon excited fluorescence in organic materials: An ultrafast coincidence detector. *J. Phys. Chem. Lett.* **2017**, *8*, 388.
- 13. Villabona-Monsalve, J. P.; Calderon-Losada, O.; Nunez Portela, M.; Valencia, A. Entangled two photon absorption cross section on the 808 nm region for the common dyes zinc tetraphenylporphyrin and rhodamine b. *J. Phys. Chem. A* **2017**, *121*, 7869–7875.
- 14. Tabakaev, D.; Montagnese, M.; Haack, G.; Bonacina, L.; Wolf, J.-P.; Zbinden, H.; Thew, R. Energy-time-entangled two-photon molecular absorption. *Phys. Rev. A* **2021**, *103*, 033701.
- 15. Tabakaev, D.; Djorovi'c, A.; La Volpe, L.; Gaulier, G.; Ghosh, S.; Bonacina, L.; Wolf, J.-P.; Zbinden, H.; Thew, R.T. Spatial properties of entangled two-photon absorption, spatial properties of entangled two-photon absorption, *Phys. Rev. Lett.* **2022**, *129*, 183601.
- 16. Dayan, B.; Pe'er, A.; Friesem, A. A.; Silberberg, Y. Two photon absorption and coherent control with broadband down-converted light. *Phys. Rev. Lett.* **2004**, *93*, 023005.
- 17. Rubin, M. H.; Klyshko, D. N.; Shih, Y. H.; Sergienko, A. V. Theory of two-photon entanglement in type-II optical parametric down-conversion. *Phys. Rev. A* **1994**, *50*, 5122–5133.
- 18. Karan, S.; Aarav, S.; Bharadhwaj H.; Taneja L.; De, A.; Kulkarni, G.; Meher, N.; Jha, A. K. Phase matching in β-barium borate crystals for spontaneous parametric down-conversion. *J. Opt.* **2022**, *22*, 083501.
- 19. Georgiades, N. P.; Polzik, E. S.; Edamatsu, K.; Kimble, H. J.; Parkins, A. S. Nonclassical excitation for atoms in a squeezed vacuum. *Phys. Rev. Lett.* **1995**, *75*, 3426–3429.
- 20. Upton, L.; Harpham, M.; Suzer, O.; Richter, M.; Mukamel, S.; Goodson, T., III. Optically excited entangled states in organic molecules illuminate the dark. *J. Phys. Chem. Lett.* **2013**, *4*, 2046–2052.
- 21. Varnavski, O.; Goodson, T., III. Two-photon fluorescence microscopy at extremely low excitation intensity: The power of quantum correlations. *J. Am. Chem. Soc.* **2020**, *142*, 12966–12975.
- 22. Varnavski, O.; Gunthardt, C.; Rehman, A.; Luker, G. D.; Goodson, T., III. Quantum light-enhanced two-photon imaging of breast cancer cells. *J. Phys. Chem. Lett.* **2022**, *13*, 2772-

- 23. Benninger, R. K. P.; Piston, D.W. Two-photon excitation microscopy for the study of living cells and tissues. *Current Protocols in Cell Biology*, **2013**, *59*, 4.11.1-4.11.24.
- 24. Schlawin, F.; Dorfman, K.E.; Mukamel, S. Entangled two-photon absorption spectroscopy. *Acc. Chem. Res.* **2018**, *51*, 2207–2214.
- 25. Szoke, S.; Liu, H.; Hickam, B.P.; He, M.; Cushing, S.K. Entangled light-matter interactions and spectroscopy. *J. Mater. Chem. C* **2020**, *8*, 10732–10741.
- 26. Burdick, R.K.; Schatz, G. C.; Goodson, T., III. Enhancing entangled two-photon absorption for picosecond quantum spectroscopy. *J. Am. Chem. Soc.* **2021**, *143*, 16930–16934.
- 27. Zhang, Z.; Peng, T.; Nie, X.; Agarwal, G. S.; Scully, M. O. Entangled photons enabled time-frequency-resolved coherent Raman spectroscopy and applications to electronic coherences at femtosecond scale. *Light Sci. Appl.* **2022**, *11*, 27.
- 28. Fu, M.; Tabakaev, D.; Thew, R.T.; Wesolowski, T. A. Fine-tuning of entangled two-photon absorption by controlling the one-photon absorption properties of the chromophore. *J. Phys. Chem. Lett.* **2023**, *14*, 2613–2619.
- 29. Giri, S. K.; and Schatz, G. C. Manipulating two-photon absorption of molecules through efficient optimization of entangled light. *J. Phys. Chem. Lett.* **2022**, *13*, 10140–10146.
- 30. Kang, G.; Nasiri Avanaki, K.; Mosquera, M. A.; Burdick, R. K.; Villabona-Monsalve, J. P.; Goodson, T., III.; Schatz, G. C. Efficient modeling of organic chromophores for entangled two-photon absorption. *J. Am. Chem. Soc.* **2020**, *142*, 10446–10458.
- 31. Raymer, M.G.; Landes, T.; Marcus, A.H. Entangled two-photon absorption by atoms and molecules: A quantum optics tutorial, *J. Chem. Phys.*, **2021**, *155*, 081501.
- 32. Landers, T.; Raymer, M.G.; Allgaier, M.; Mercouche, S.; Smith, B.; Marcus, A.H. Quantifying the enhancement of two-photon absorption due to spectral-temporal entanglement, *Opt. Express*, **2021**, *29*, 20022-20033.
- 33. Parzuchowski, K.M.; Mikhaylov, A.; Mazurek, M.D.; Wilson, R.N.; Lum, D.J.; Gerrits, T.; Camp Jr., C.H.; Stevens, M.J.; Jimenez, R. Setting bounds on entangled two-photon absorption cross sections in common fluorophores, *Phys. Rev. Applied.*, **2021**, *15*, 044012.

- 34. Landes, T.; Allgaier, M.; Merkouche, S.; Smith, B.J.; Andrew H. Marcus, A.H.; Raymer, M.G. Experimental feasibility of molecular two-photon absorption with isolated time-frequency-entangled photon pairs *Phys.Rev. Res.* **2021**, *3*, 033154.
- 35. He, M.; Hickam, B. P.; Nathan Harper, N.; Cushing, S.K. Experimental upper bounds for resonance-enhanced entangled two-photon absorption cross section of indocyanine green *J. Chem. Phys.* **2024**, *160*, 094305.
- 36. Corona-Aquino, S.; Calderon-Losada, O.; Li-Gomez, M. Y.; Cruz-Ramirez, H.; Alvarez Venicio, V.; Carreon-Castro, M. d. P.; de J. Leon-Montiel, R.; U'Ren, A. B. Experimental study of the validity of entangled two-photon absorption measurements in organic compounds. J. *Phys. Chem. A* **2022**, 126, 2185–2195.
- 37. Hickam, B. P.; He, M.; Harper, N.; Szoke, S.; Cushing, S. K. Single-photon scattering can account for the discrepancies among entangled two-photon measurement techniques. *J. Phys. Chem. Lett.* **2022**, *13*, 4934–4940.
- 38. Mikhaylov, A.; Wilson, N. R.; Parzuchowski, M. K.; Mazurek, D. M. et al., Hot-band absorption can mimic entangled two-photon absorption, *J. Phys. Chem. Lett.* **2022**, 13, 1489.
- 39. Varnavski, O.; Giri, S. K.; Chiang, T.; Zeman IV, C. J.; Schatz, G. C.; Goodson, T., III. Colors of entangled two-photon absorption. *Proc. Natl. Acad. Sci.* (*USA*) **2023**, *120*, e2307719120.
- 40. Förtsch, S.; Mena-Osteritz, E.; Bäuerle, P. Synthesis and characterization of β, B'-dimethylated dithieno [3,2- b:2',3'-d] pyrroles and their corresponding regioregular conducting electropolymers. *Polym. Chem.* **2021**, *12*, 3332–3345.
- 41. Pron, A.; Reghu, R. R.; Rybakiewicz, R.; Cybulski, H.; Djurado, D.; Grazulevicius, J. V.; Zagorska, M.; Kulszewicz-Bajer, I.; Verilhac, J.-M. Triarylamine substituted arylene bisimides as solution processable organic semiconductors for field effect transistors. Effect of substituent position on their spectroscopic, electrochemical, structural, and electrical transport properties. *J. Phys. Chem. C* **2011**, *115*, 15008–15017.
- 42. Pluczyk, S.; Zassowski, P.; Rybakiewicz, R.; Wielgosz, R.; Zagorska, M.; Lapkowski, M.; Pron, A. UV-Vis and EPR Spectroelectrochemical investigations of triarylamine functionalized arylene bisimides. *RSC Adv.* **2015**, *5*, 7401–7412.
- 43. Sefer, E.; Baycan Koyuncu, F. Naphthalenediimide bridged D-A polymers: Design, synthesis and electrochromic properties. *Electrochim. Acta* **2014**, *143*, 106–113.

- 44. Chen, Z.; Xu, D.; Zhu, M.; Wang, Y.; Feng, J.; Shu, C.; Xiao, S.; Meng, J.; He, J. Gigantic blue shift of two-photon-induced photoluminescence of interpenetrated metal-organic framework (MOF). *Nanophotonics* **2023**, *12*, 3781–3791.
- 45. Eshun, A.; Cai, Z.; Awies, M.; Yu, L.; Goodson III, T. Investigations of thienoacene molecules for classical and entangled two-photon absorption. *J. Phys. Chem. A* **2018**, *122*, 8167–8182.
- 46. Villabona-Monsalve, J. P.; Tcyrulnikov, N. A.; Lorenzo, E. R.; LaBine, N.; Burdick, R.; Krzyaniak, M. D.; Young, R. M.; Wasielewski, M. R.; Goodson, T., III. Two-photon absorption in electron donor–acceptor dyads and triads using classical and entangled photons: Potential systems for photon-to-spin quantum transduction *J. Phys. Chem. C* 2022, *126*, 6334–6343.
- 47. Villabona-Monsalve, J. P.; Burdick, R. K.; Goodson III, T. Measurements of entangled two-photon absorption in organic molecules with CW-pumped type-I spontaneous parametric down-conversion. *J. Phys. Chem. C.* **2020**, *124*, 24526-24532.